

Ethylene-Bridged Bis(amidines)

Ethylene-Bridged Tetradentate Bis(amidines): Supramolecular Assemblies through Hydrogen Bonding and Photoluminescence upon Deprotonation

Alvaro Calderón-Díaz,^[a] Janet Arras,^[a] Ethan T. Miller,^[a] Nattamai Bhuvanesh,^[b] Colin D. McMillen,^[c] and Michael Stollenz*^[a]

Dedicated to Professor Uwe Rosenthal on the occasion of his 70th birthday

Abstract: Sterically crowded tetradentate bis(amidines) encapsulate their N–H functionalities or unveil them to undergo inter- and intramolecular hydrogen bonding both in solid state and solution, depending on a subtle interplay between the amidine backbone substituents. X-ray crystallography reveals for four distinct *ZZ(syn/syn)* and *EE(syn/syn)* bis(amidines) that bulky terminal *N*-Mes groups in combination with N_2C-tBu or N_2C-Ph substituents result in steric protection of the N–H moieties, whereas less crowded terminal *p*- $tBu(C_6H_4)$ groups either show encapsulation (N_2C-tBu) or hydrogen bonding (N_2C-Ph), the lat-

ter resulting in a bis(amidine) dimer formed by inter- and intramolecular hydrogen bonds. Moreover, a supramolecular solvent adduct consisting of one bis(amidine) and four ethanol molecules is presented. DFT calculations show that both the dimerization and formation of the solvent adduct is associated with a significant energy gain (dimerization: $\Delta E = -27.7$ kcal/mol; formation of ethanol adduct: $\Delta E = -64.3$ kcal/mol). The corresponding four Li bis(amidates) are weakly blue to green-emissive in THF solution. Overall, a new series of highly flexible bis(amidines) has been examined.

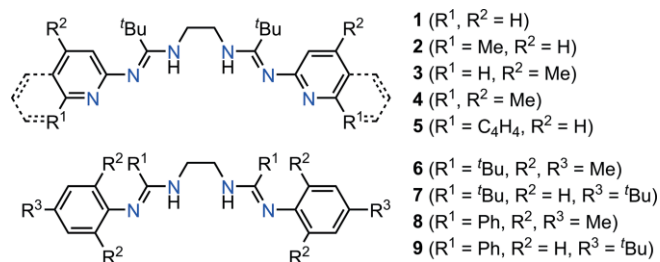
Introduction

Amidines represent a versatile class of isoelectronic *N*-analogs of carboxylic acids and esters. They have attracted considerable attention as medical and biochemical reagents, as building blocks for redox-switchable chromophores/fluorophores, and also as important ligands in coordination chemistry.^[1–3] Associated applications include homogeneous catalysis^[3] as well as utilizing amidinate complexes of transition^[4] and rare earth metal^[3e,3h] amidinates as precursors for producing thin metal/metal oxide films by atomic layer deposition (ALD).

Although known since the early 1950s,^[5] tethered bis(amidines) remained underrepresented in the literature until their striking analogy to bis(cyclopentadienyl) ligand scaffolds in “constrained” *ansa* metallocenes became apparent.^[6] In particular, bis(amidines) linked to alkylene and arylene backbones have been identified as excellent ligands for alkali metal, lanthanide, and Group 4 metal complexes,^[7,8] some of which

mediate catalytic ring-opening polymerizations/copolymerizations of cyclic esters^[9,10] and amidations of aldehydes with amines.^[11] Tetradentate bis(amidines) are also capable of embedding multiple late transition metal ions.^[12–14]

We have recently presented a new class of flexible ethylene-linked bis(amidines) **1–5** that bear additional terminal *N*-donor sites (Figure 1).^[15] These aromatic variants of the closely related and extremely versatile bridged 1,3,5-triazapentadienes^[16] feature variable *inter*- and *intramolecular* NH...N' hydrogen bonds in the solid state that are also preserved in solution (Figure 1). Upon deprotonation using $nBuLi$ or $NaN(SiMe_3)_2$, the corresponding blue-light emitting bis(amidates) [**1–5**Li]₂ are formed in THF solution.

Figure 1. Ethylene-bridged *N,N'*-disubstituted bis(amidines) **1–9**.

Our ongoing interest in tetradentate bis(amidines) has arisen from designing a suitable ligand framework for defined linear Cu^I cluster assemblies^[17] that were obtained from **8** and mesitylcopper.^[18]

[a] A. Calderón-Díaz, Dr. J. Arras, E. T. Miller, Prof. Dr. M. Stollenz
Department of Chemistry and Biochemistry, Kennesaw State University,
370 Paulding Avenue NW, MD1203, Kennesaw, GA 30144, USA
E-mail: Michael.Stollenz@kennesaw.edu
<http://facultyweb.kennesaw.edu/mstollen/>

[b] Department of Chemistry, Texas A&M University,
580 Ross Street, P.O. Box 30012, College Station, TX 77842-3012, USA

[c] Department of Chemistry, Clemson University,
379 Hunter Laboratories, Clemson, SC 29634-0973, USA

Supporting information and ORCID(s) from the author(s) for this article are available on the WWW under <https://doi.org/10.1002/ejoc.202000207>.

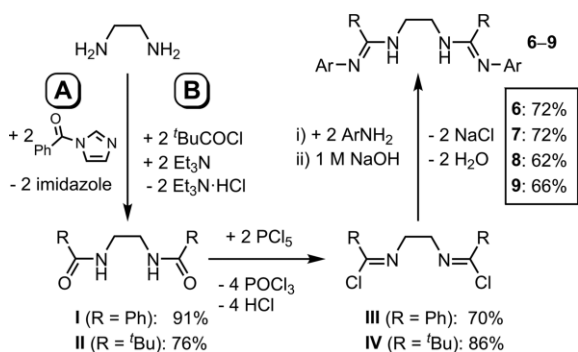
Part of the French Chemical Society DCC Prizewinner Collection.

Although ethylene-bridged bis(amidines) were the first reported examples of tetradentate bis(amidines) interconnected by a flexible alkylene linker,^[5] still little is known about their molecular structures both in solid state and solution. Only the related *trans*-1,2-diaminocyclohexane-linked tetradentate (*t*-1,2-DACH)-bis(amidines) have been in the focus of two earlier reports.^[7] No accompanying computational studies have been published yet.

This report focuses on the synthesis and molecular structures of the new tetradentate bis(amidines) **6**, **7**, and **9** that exhibit sterically encapsulated amidine moieties or NH groups amenable to form remarkable networks of *inter*- and *intramolecular* NH...N' hydrogen bonds in the solid state, depending on the nature of the amidine substituents (Figure 1). An example of a supramolecular solvent adduct (**9**-EtOH) is also presented. Moreover, we found strong evidence for hydrogen bonding retained in solution for bis(amidine) **9** that shows hydrogen bonding in the solid state. A comprehensive computational study (gas phase) supports these observations. Similar to the hexadentate bis(amidines) **1–5**, also their tetradentate congeners **6–9** become emissive in THF solutions upon deprotonation through ⁿBuLi – a phenomenon that has never been reported for simple bis(amidines) of this kind yet.

Results and Discussion

The synthesis of **6–9** followed a proven three-step protocol (Scheme 1).^[15,17] Two benzoylation methods of ethylenediamine (**A** and **B**) were identified to provide the diamides **I** and **II** in excellent yields (up to 91 %). Chlorination using PCl₅ afforded the bis(imidoyl chlorides) **III** and **IV** (yields: 70–86 %) that were subjected to aminolysis with the corresponding arylamines to afford the target bis(amidines) **6–9** as microcrystalline solids in good yields (62–72 %).



Scheme 1. Three-step synthesis of **6–9** (**6**: R = ^tBu, Ar = Mes; **7**: R = ^tBu, Ar = *p*-^tBu(C₆H₄); **8**: R = Ph, Ar = Mes; **9**: R = Ph; Ar = *p*-^tBu(C₆H₄)).

The ¹H NMR spectra of the tetradentate bis(amidines) **6**, **7**, and **9** (recorded in CDCl₃, C₆D₆, and [D₆]DMSO, respectively) each show one set of sharp resonances for all C–H protons that suggest the presence of one tautomeric form in solution (see Table S7 and Figures S13–S31 in the Supporting Information, SI). The bulky ^tBu groups attached to the amidine moieties are indicated by sharp singlets between $\delta = 1.09$ and 1.20 ppm, thus suggesting fast rotation.

Compared to the more electron-deficient bis(amidines) **8** and **9**, the CH₂ and NH signals of **6** and of **7** are substantially upfield-shifted by up to 1.44 ppm (CH₂) and 3.37 ppm (NH), respectively. Only the N–H peak of **7** is very broad in the CDCl₃ ($\delta = 4.53$ ppm) and in the C₆D₆ spectra ($\delta = 4.61$ ppm) whereas **6** indicates only slight line broadening in C₆D₆ (at $\delta = 3.91$ ppm), accompanied by an upfield-shift of about 0.1 ppm for that signal, in comparison with the CDCl₃ spectrum. This is in clear contrast to bis(amidine) **8** that produces broad resonance signals in its C₆D₆-¹H NMR spectrum at room temperature.^[17] Additional broadened signals at $\delta = 3.02$, 5.72, and 7.89 ppm were found and suggest that C=N double-bond stereoisomers (*EE*, *EZ/ZE*, and *ZZ*) and their *syn/anti* rotational isomers (**c**) exist in solution. These isomers can interconvert through tautomerism (**a**) and C–N single-bond rotation (**b**) at the amidine moieties (Scheme 2).

If the predominant tautomer retains the –NH(CH₂)₂NH– diamine core motif, then eight distinct and four additional pairs of identical stereoisomers are possible for ethylene-bridged *N,N'*-disubstituted bis(amidines). This was confirmed for the solid state by the XRD structures of **1–5**,^[15] **6**, **7**, **8**,^[17] **9**·0.8CH₂Cl₂, and **9**-EtOH that all show the ethylenediamine tautomeric form (*vide infra*).

The underlying prototropic exchange is considerably suppressed in **8** if [D₆]DMSO is used, as only one set of resonance signals becomes apparent.^[17] For **6**, **7**, and **9**, line width of the broad N–H resonance signals decreases significantly in [D₆]DMSO and they are also downfield-shifted by 1.71 ppm (**6**), 1.04 ppm (**7**), 1.76 ppm (**8**),^[17,19] and 1.41–1.46 ppm (**9**),^[20] if compared to their respective ¹H NMR spectra in the least polar solvent (C₆D₆) within this series (Table S7). Most evidently, the N–H signal of **9** in C₆D₆ shows a notable downfield shift (by up to 0.60 ppm) in comparison with **8**.^[19] This difference in chemical shift is more pronounced than for the CH₂ resonances ($|\Delta\delta| = 0.13$ ppm)^[21] and the phenyl group proton signals ($|\Delta\delta| \approx$ up to 0.1 ppm) of **8** and **9**. Therefore, sole electronic effects of the terminal aryl substituents are not exclusively responsible for the large difference between the N–H shifts. Similar to the hexadentate bis(amidines) **1–5**,^[15] the large $|\Delta\delta|$ value strongly suggests the presence of hydrogen bonds in solution.^[22] The deshielding effect of hydrogen bonds is more distinct in less polar C₆D₆ than in CDCl₃ or [D₆]DMSO, as the latter two serve as potential hydrogen-bond donor/acceptors. Temperature-dependent ¹H NMR spectra of **9** in CDCl₃ show increased deshielding of the N–H protons with decreasing temperature (by +0.67 ppm from 27 °C to –60 °C), which is also consistent with the formation of hydrogen bonds in solution (Figure S31).

X-ray crystallography confirmed hydrogen bonding for the solid-state structure of **9** and the existence of hydrogen bonds in solution was supported by density functional theory (DFT) calculations (*vide infra*).

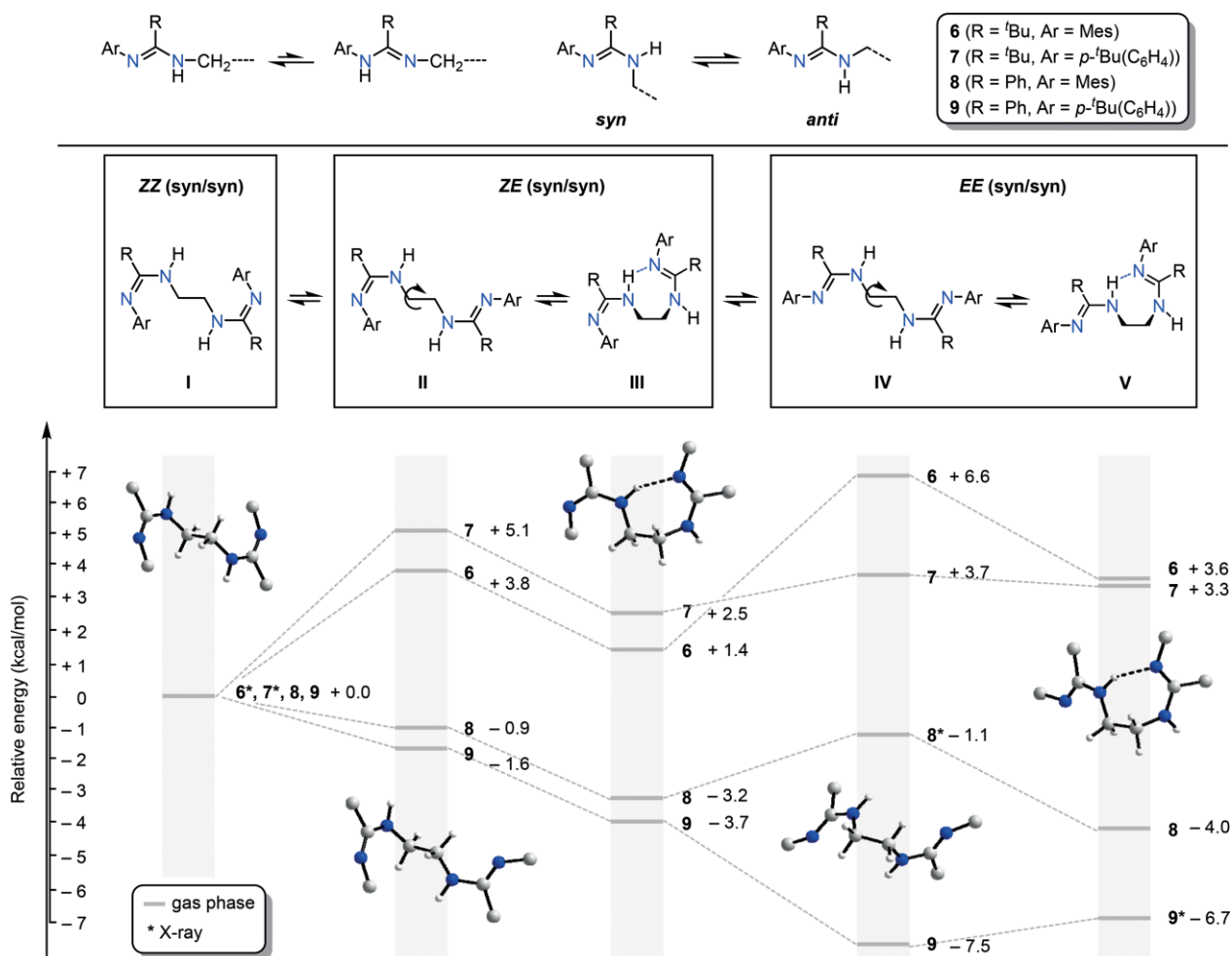
The ¹³C{¹H} NMR spectra of **6** and **7** in all three deuterated solvents are very similar and show the diagnostic signals of the common –N=C(^tBu)NH(CH₂)₂NH(^tBu)C=N– core motif at $\delta = 28.8$ –29.4, 38.3–39.0 (^tBu), 42.0–44.3 (CH₂), and 158.0–160.9 ppm (amidine signal, Table S8). Notably, the CH₂ resonance of **7** is clearly broader than of **6**, which is consistent with

the corresponding broader proton signals of **7** in CDCl_3 , C_6D_6 , and $[\text{D}_6]\text{DMSO}$, respectively. Bis(amidines) **8** and **9** show similar CH_2 shifts ($\delta = 40.6\text{--}43.7$ ppm) and similar quaternary carbon signals of the amidine moieties ($\delta = 155.5\text{--}158.4$ ppm).

In order to enlighten the structural features of **6**, **7**, and **9** in the solid state, single crystals were grown and subjected to X-ray crystallographic structure determinations. Suitable single crystals of **6** and **7** were obtained from hexanes solutions (see Experimental Section). The results for **6** and **7** are shown in Figure 2, Figures S1–S6, and Table S1; key crystallographic distances and angles are outlined in Table S3. In contrast to the previously reported solid-state *EE* (*syn, syn*) form of bis(amidine) **8**, the XRD analyses reveal that **6** and **7** exclusively exist as *ZZ* (*syn, syn*) stereoisomers in the crystalline state. This is consistent with the increased steric repulsion between the terminal aryl substituents and the bulky *tert*-butyl group. Similar to **8**, the bulky substituents of the amidine components of **6** and **7** also hamper the formation of intramolecular hydrogen bonds that were earlier observed in the less crowded hexadentate bis(amidines) **1–5**.^[15]

Single crystals of **9** suitable for XRD analysis were isolated from a concentrated CH_2Cl_2 solution (the result is shown in Figure 2, Figures S7–S9, and Table S2). This bis(amidine) crystallizes as a solvate $\mathbf{9}\cdot 0.8\text{CH}_2\text{Cl}_2$, without any significant hydrogen bonding interactions between CH_2Cl_2 and the bis(amidine) moieties (Figure S9; closest donor/acceptor distance for $\text{N}\cdots\text{H}\cdots\text{Cl}$ is $3.780(3)$ Å). However, as opposed to **6–8**, bis(amidine) **9** does form *intramolecular* hydrogen bonds between the two tethered amidine compartments to constitute a seven-membered ring. In addition, *intermolecular* hydrogen bonds are observed between two molecular entities forming a 14-membered ring within the resulting C_i -symmetrical dimer of **9**. This phenomenon was earlier observed for a tetradentate (*t*-1,2-DACH)-bis(amidine)^[7a] and the hexadentate congener **5**.^[15] Recently, a related bis(guanidine) featuring an *n*-propylene bridge has been reported that shows inter- and intramolecular hydrogen bonding as well.^[23]

According to Jeffery's classification,^[26] all hydrogen bonds of **9** can be considered as being moderately strong ($\text{N}_{\text{NH}}\cdots\text{N}=\text{C}$: $2.86\text{--}3.06$ Å; $\text{NH}\cdots\text{N}$: $2.12\text{--}2.21$ Å; $\text{N}\cdots\text{H}\cdots\text{N}$ angles of $141\text{--}161^\circ$



Scheme 2. a: Tautomerism in **6–9**; b: *syn/anti* rotational isomers through C–N single-bond rotation; c: *ZZ* (*syn/syn*), *ZE/EE* (*syn/syn*), and *EE* (*syn/syn*) isomers of **6–9** including two rotational isomers, **III** and **V**, that show intramolecular hydrogen bonds and their relative stability (kcal/mol) in the gas phase. Structure representations denoted with an asterisk are geometry-optimized structures based on X-ray data. The remaining 13 *syn/anti* and *anti/anti* rotational isomers that correspond to **I**, **II**, and **IV**^[24] are not shown.^[25] The computed structures of **I–V** depicted are the rotational isomers of **6** as representative examples for **6–9**. See SI for more information.

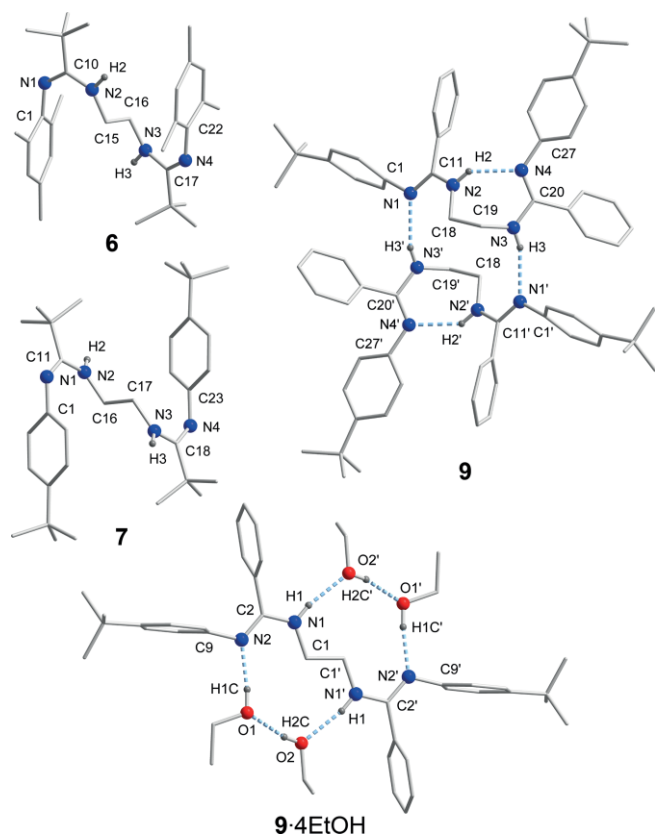


Figure 2. XRD molecular structures of **6**, **7**, **9**, and **9·4EtOH**.

(Table S5). Consequently, the IR $\nu(\text{N-H})$ stretching frequency of **9** (3272 cm^{-1}) is redshifted by $132\text{--}175\text{ cm}^{-1}$ relative to the bis(amidines) **6–8** that do not show evidence of hydrogen bonding in the solid state (Table S6). This is in turn consistent with the $\nu(\text{N-H})$ values of **1–5** as these have hydrogen bonds which lie in a similar range ($3252\text{--}3309\text{ cm}^{-1}$).^[15]

The fragile network of hydrogen bonds is susceptible to alternative hydrogen-bond donor/acceptor molecules, as demonstrated by the formation of solvent adduct **9·4EtOH** (see Figure 2 Figures S10–S12, and Table S2).

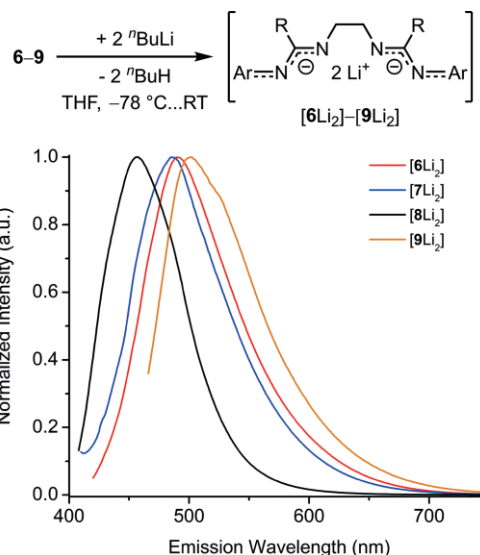
This supramolecular assembly was obtained by recrystallization of **9** from a mixture of ethanol and acetonitrile (see Experimental Section). Both amidine units accept overall four ethanol molecules in an approximate D_{2h} -symmetrical arrangement; two of which are undergoing intermolecular $\text{O-H}\cdots\text{O}$ hydrogen bonding interconnect the amine NH donor of one amidine compartment with the imine acceptor of the second one through $\text{N-H}\cdots\text{O}$ and $\text{O-H}\cdots\text{N}$ hydrogen bonds. This gives rise to two 11-membered rings. While all hydrogen bonds in **9·4EtOH** are moderately strong, the $\text{O-H}\cdots\text{O}$ and $\text{O-H}\cdots\text{N}$ bonds are significantly shorter (by up to 0.09 \AA) than the $\text{N-H}\cdots\text{O}$ bonds (Table S5). The pronounced N-C single bond character of the central $\text{-NH}(\text{CH}_2)_2\text{NH-}$ diamine bridge gives rise to large Δ_{CN} parameters^[1, 27] for **6–8** ($0.073\text{--}0.956\text{ \AA}$, Table S4). Bis(amidinate) **9** and its solvent adduct **9·4EtOH** have clearly smaller values (0.059 and 0.0602 \AA), thus indicating an influence of hydrogen bonding on increased delocalization within the amidine moieties. The impact of E/Z isomerization on the N=C-NH

angles of **6–9** and **9·4EtOH** is substantial – they are larger by $6\text{--}10^\circ$ in the ZZ isomers than in the EE isomers. This is consistent with the increased steric constraints on the amidine moieties in the ZZ isomers, as observed for **6** and **7**.

The relative stability (kcal/mol) for the molecular structures of **6–9** (single-crystal X-ray structures **I**, **IV** and **V** and additional ZE (syn/syn) isomers **II** and **III**) was modeled in the gas phase using DFT at the RI-B3LYP-D3/def2-TZVP level of theory (Scheme 2; see the SI for more information).

This study helps us to understand which rotational isomers could be accessible in solution and if the internal hydrogen bonding in **III** and **V** would give stability preferences. For **6** and **7**, the compounds with the bulky $t\text{Bu}$ substituents (ZZ (syn/syn) isomer **I**) is energetically favored (in the gas phase by 6.6 kcal/mol (**6**) and 3.7 kcal/mol (**7**) over **IV**, and by 3.8 kcal/mol (**6**) and 5.1 kcal/mol (**7**) over **II**) as evidenced by XRD analysis and predicted by DFT calculations. The less bulky Ph substituent in **8** and **9** results in lower energies of the EE (syn/syn) isomers **IV** (**8**) and **V** (**9**) (in the gas phase by 1.1 kcal/mol (**8**) and 6.7 kcal/mol (**9**) in relation to **I**, and by 0.2 kcal/mol (**8**) and 5.1 kcal/mol (**9**) in relation to **II**). In the gas phase for **9**, form **IV** is the lowest energy structure (by about 0.8 kcal/mol energetically favored over **V**). For all isomers **II–V**, **8** is higher in energy than **9**. In order to understand the effect of the intermolecular hydrogen bonding in **9**, we calculated the dimerization energy and the formation of **9·4EtOH** from **9** + 4 EtOH. Both reactions are significantly exothermic (dimerization: $\Delta E = -27.7\text{ kcal/mol}$; formation of **9·4EtOH**: $\Delta E = -64.3\text{ kcal/mol}$).

The unexpected photoluminescence behavior of the hexadentate bis(amidates) [**1–5**Li₂] encouraged us to examine the corresponding Li complexes of **6–9**.^[15] There are only a few examples of isolated Li complexes with tetradentate bis(amidates) described in the literature and no photophysical properties have been reported yet.^[7,8c–8e,8j] To our surprise, the tetradentate bis(amidines) **6–9** become weakly emissive in THF solution upon deprotonation using $n\text{BuLi}$ to form [**6–9**Li₂] (Scheme 3).



Scheme 3. Deprotonation of **6–9** and steady-state emission spectra of [**6–9**Li₂] in THF.

The steady-state photoluminescence spectra of [6–9Li₂] show emission maxima between 456–502 nm that are clearly redshifted (by up to 81 nm), in relation to [1–5Li₂] (Figure S40–S43, Table S35, and Ref. 15). The Stokes shifts of [6Li₂] (0.50 eV) and [7Li₂] (0.55 eV) are comparable to [1–4Li₂], whereas the aryl-substituted bis(amidates) [8Li₂] and [9Li₂] have smaller values (0.40 eV and 0.25 eV, respectively), tending to be similar to the enhanced-conjugated Li bis(amidate) [5Li₂] (0.16 eV). This further supports our initial hypothesis that the bis(amidate) moiety is the origin of the emission in THF solution, which is predominantly affected by the individual amidate substituents.

Conclusion

Three new ethylene-bridged tetradentate bis(amidines), **6**, **7**, and **9**, were reported. X-ray crystallography reveals that these bis(amidines) form either distinct *ZZ(syn/syn)* isomers in the solid state if bulky ^tBu groups serve as central substituents or *EE(syn/syn)* isomers, if Ph substituents are incorporated into the bis(amidine) scaffold. DFT calculations support this observation for the gas phase. While the N–H functional groups of **6**, **7**, and the closely related bis(amidine) **8** are encapsulated in the sterically protected amidine compartments, **9** shows a versatile network of *intra*- and *intermolecular* hydrogen bonds. Hydrogen bonding of **9** is retained in solution, which was confirmed by significant NH-proton downfield shifts in the ¹H NMR spectra and supported by DFT gas phase calculations. Moreover, **9** is capable of forming supramolecular assemblies with protic solvents such as ethanol, as demonstrated by the solvent adduct **9**·4EtOH. All bis(amidines) **6–9** form weakly luminescent Li bis(amidinato) complexes [6–9Li₂] through deprotonation in THF solution. Ongoing studies and future projects will be devoted to explore the versatile coordination chemistry of **6–9** with respect to new photoluminescent materials.

Experimental Section

General methods: All synthetic procedures involving air- and moisture-sensitive compounds were carried out by using Schlenk techniques under an atmosphere of dry argon. Glassware was heat-sealed with a heat gun under vacuum.

Solvents: Prior to use, tetrahydrofuran (THF), diethyl ether, and toluene were freshly distilled from sodium/benzophenone. CH₂Cl₂ was distilled from CaH₂. Alternatively, the aforementioned solvents were purified using a PPT Solvent Purification System. For non-inert manipulations, CH₂Cl₂, diethyl ether, and hexanes (mixture of isomers) were used as received without further purification.

Deuterated solvents: CDCl₃ (Cambridge Isotope Laboratories, Inc., D, 99.8 % + 0.03 % v/v tetramethylsilane, TMS), C₆D₆ (Cambridge Isotope Laboratories, Inc., D, 99.5 %), and [D₆]DMSO (Cambridge Isotope Laboratories, Inc., D, 99.9 %) were used as received without further purification.

Reactants: Triethylamine (Alfa Aesar, 99 %) was distilled from sodium before use. Ethylene diamine (Alfa Aesar, >99 %), pivaloyl chloride (Acros, 99 %), benzoic acid (Alfa Aesar, 99 %), *N,N'*-carbonyldiimidazole (Oakwood Chemical, 98+%), PCI₅ (Alfa Aesar, 98 %), mesitylamine (TCI, >99 %), *p*-*tert*-butylaniline (Oakwood Chemicals,

98 %), and *n*-butyllithium (Acros, 1.6 M in hexanes) used as received without further purification. The syntheses of *N,N'*-1,2-ethanediybis(2,2-dimethylpropanimidoyl chloride)^[15] and **8**^[17] were previously described.

Elemental analyses were performed by Atlantic Microlab, Inc. Melting points were determined with an SRS (Stanford Research Systems) Digi Melt instrument using open capillaries; values are uncorrected (the heating rate was 2 K/min). NMR measurements were recorded on a Bruker Avance III 400 spectrometer at ambient probe temperatures unless otherwise noted. ¹³C{¹H} NMR resonances were obtained with proton broadband decoupling and referenced to the solvent signals of [D₆]DMSO at 39.5, CDCl₃ at 77.0, and C₆D₆ at 128.0 (¹H NMR: 2.50 (DMSO), 7.24 (CHCl₃), and 7.15 (benzene), respectively). ¹³C{¹H} NMR assignments are based on DEPT 135, and the following 2D experiments: COSY, NOESY, HSQC, and HMBC. Mass-spectrometric analyses were performed on a Waters Q-ToF API US quadrupole time of flight MS system (low resolution ESI) and on a Thermo Orbitrap Velos Pro MS system (high resolution ESI). IR spectra were measured on a PerkinElmer Spectrum One FT-IR Spectrometer equipped with a Universal ATR Sampling Accessory. UV/Vis spectra of solutions of **6–9** and [6–9Li₂] in THF were measured with a Cary 60 spectrometer. Steady-state emission spectra of solutions of [6–9Li₂] in THF were recorded on a PTI Picomaster 1 fluorescence spectrometer system.

Synthesis of *N,N'*-1,2-ethanediybis(benzenecarboximidoyl chloride): This compound was prepared in analogy to a method described earlier, with modifications.^[17] *N,N'*-1,2-ethanediybis(benzamide) (9.887 g, 36.85 mmol) and PCI₅ (15.347 g, 73.70 mmol) were suspended in CH₂Cl₂ (100 mL) with stirring to give a clear yellow solution. After 3 d, triethylamine (10.3 mL, 7.48 g, 73.9 mmol) was added dropwise via syringe over a period of 5 min to form a colorless precipitate. The suspension was reduced to 40 mL in oil pump vacuum and filtered. The filter cake was washed with diethyl ether (3 × 10 mL). Additional diethyl ether (30 mL) was added to the filtrate to form more colorless precipitate. This was removed by filtration and the filter cake was washed with cold (0 °C) diethyl ether (3 × 10 mL). The filtrate was reduced to dryness using oil pump vacuum, then redissolved in CH₂Cl₂ (20 mL), and finally stored at –35 °C. After 2 d, pale yellow crystals formed that were isolated by filtration, rinsed with cold (–78 °C) CH₂Cl₂ (3 × 3 mL), and dried in oil pump vacuum for 18 h to yield a light yellow powder. Yield: 7.918 g (25.94 mmol, 70 %).

General Procedure for the Preparation of **6, **7**, and **9**:** A solution of arylamine (19.42 mmol; **9**: 5.88 mmol) in toluene (10 mL) was added dropwise to a solution of *N,N'*-1,2-ethanediybis(2,2-dimethylpropanimidoyl chloride) (9.80 mmol; **9**: 2.94 mmol) in toluene (40–50 mL) with stirring. The reaction mixture was heated to reflux for 24 h, and then cooled to room temperature, and filtered. The filter cake was first washed with cold (0 °C) toluene (3–5 × 10 mL), then with diethyl ether (3 × 5 mL), and finally suspended in a mixture of diethyl ether (50 mL) and a saturated aqueous Na₂CO₃ solution (50 mL) which was stirred for 30 min. The organic phase was separated, washed with water (3–5 × 100 mL; **9**: 3 × 25 mL), and dried with anhydrous Na₂SO₄. Subsequent filtration, removal of all volatiles from the filtrate by rotary evaporation resulted in a colorless solid that was recrystallized from hexanes (**6–9**) or from a mixture of CH₂Cl₂ and diethyl ether (1:1 v/v) and dried in oil pump vacuum for 14–24 h.

Synthesis of **6:** This bis(amidine) was obtained by recrystallization from hexanes at 5 °C within 2 d as a colorless crystalline solid. Yield: 72 %; Mp: 95.3–96.4 °C. Anal. Calcd for C₃₀H₄₆N₄: C, 77.87; H, 10.02; N, 12.11; found C, 77.95; H, 10.29; N, 12.08. ¹H NMR (400.1 MHz,

CDCl₃): δ = 1.20 (s, 18 H, CH₃, ^tBu), 1.98 (s, 12 H, CH₃, *o*-Mes), 2.18 (s, 6 H, CH₃, *p*-Mes), 2.45 (s, 4 H, CH₂), 4.05 (broad s, 2 H, NH), 6.68 (s, 4 H, CH). ¹H NMR (400.1 MHz, C₆D₆): δ = 1.12 (s, 18 H, CH₃, ^tBu), 2.11 (s, 12 H, CH₃, *o*-Mes), 2.21 (s, 6 H, CH₃, *p*-Mes), 2.42 (broad s, 4 H, CH₂), 3.91 (broad s, 2 H, NH), 6.77 (s, 4 H, CH). ¹H NMR (400.1 MHz, [D₆]DMSO): δ = 1.15 (s, 18 H; CH₃, ^tBu), 1.86 (s, 12 H; CH₃, *o*-Mes), 2.12 (s, 6 H; CH₃, *p*-Mes), 2.35 (broad s, 4H; CH₂), 5.62 (broad s, 2H; NH), 6.59 (s, 4H; CH). ¹³C{¹H} NMR (100.6 MHz, CDCl₃): δ = 18.3 (CH₃, *o*-Mes), 20.6 (CH₃, *p*-Mes), 29.1 (CH₃, ^tBu), 38.5 (C, ^tBu), 43.0 (CH₂), 126.9 (C, *o*-Mes), 127.8 (CH), 129.8 (C, *p*-Mes), 145.3 (C, *i*-Mes), 158.4 (C, CN₂). ¹³C{¹H} NMR (100.6 MHz, C₆D₆): δ = 18.7 (CH₃, *o*-Mes), 20.9 (CH₃, *p*-Mes), 29.1 (CH₃, ^tBu), 38.7 (C, ^tBu), 43.4 (CH₂), 126.8 (C, *o*-Mes), 128.4 (CH), 129.5 (C, *p*-Mes), 146.3 (C, *i*-Mes), 158.0 (C, CN₂). ¹³C{¹H} NMR (100.6 MHz, [D₆]DMSO): δ = 18.1 (CH₃, *o*-Mes), 20.3 (CH₃, *p*-Mes), 28.9 (CH₃, ^tBu), 38.5 (C, ^tBu), 42.0 (CH₂), 125.7 (C, *o*-Mes), 127.3 (CH), 127.6 (C, *p*-Mes), 145.9 (C, *i*-Mes), 158.1 (C, CN₂). MS (ESI(+)): *m/z* (relative intensity): 463 (13) [M + H]⁺, 232 (100) [M + 2 H]²⁺. HRMS (ESI(+)): *m/z* calcd. for C₃₀H₄₇N₄ [M + H]⁺ 463.3801, found 463.3792. IR (neat, cm⁻¹): $\tilde{\nu}$ = 3447 (w, ν (N-H)), 2961, 2941, 2919, 2909 (m, ν (C-H)), 2864 (w, ν (C-H)), 2730 (w), 1644 (vs), 1604 (m), 1513, 1474 (s), 1451, 1435, 1393, 1374, 1362 (m), 1300 (w), 1279, 1266 (m), 1226 (s), 1179 (m), 1139 (w), 1035, 1007 (m), 936 (w), 898, 882 (m), 856 (s), 825 (w), 767, 760 (m), 710 (s). UV/Vis (THF): λ [nm] (ϵ [L · mol⁻¹ · cm⁻¹]) 243, 1.92 × 10⁴; ≈294, 4.83 × 10³ (br shoulder).

Synthesis of 7: This bis(amidine) was obtained by recrystallization from hexanes at 5 °C within 3 d as a colorless crystalline solid. Yield: 72 %; Mp: 159.5–161.0 °C. Anal. Calcd for C₃₂H₅₀N₄: C, 78.31; H, 10.27; N, 11.42; found C, 78.40; H, 10.36; N, 11.46. ¹H NMR (400.1 MHz, CDCl₃): δ = 1.14 (s, 18 H; CH₃, ^tBu-CN₂), 1.26 (s, 18 H; CH₃, ^tBu-C₆H₄), 2.80 (broad s, 4 H; CH₂), 4.53 (broad s, 2 H; NH), 6.63 (d, ³J_{H,H} = 8.0 Hz, 4 H; CH, *m*-C₆H₄), 7.16 (d, ³J_{H,H} = 7.4 Hz, 4 H; CH, *o*-C₆H₄). ¹H NMR (400.1 MHz, C₆D₆): δ = 1.11 (s, 18 H; CH₃, ^tBu-CN₂), 1.28 (s, 18 H; CH₃, ^tBu-C₆H₄), 2.84 (s, 4 H; CH₂), 4.61 (broad s, 2 H; NH), 6.91 (d, ³J_{H,H} = 7.7 Hz, 4 H; CH, *m*-C₆H₄), 7.24 (d, ³J_{H,H} = 7.9 Hz, 4 H; CH, *o*-C₆H₄). ¹H NMR (400.1 MHz, [D₆]DMSO): δ = 1.09 (s, 18 H; CH₃, ^tBu-CN₂), 1.23 (s, 18 H; CH₃, ^tBu-C₆H₄), 2.54 (s, 4 H; CH₂), 5.65 (broad s, 2 H; NH), 6.45 (d, ³J_{H,H} = 7.8 Hz, 4 H; CH, *m*-C₆H₄), 7.11 (d, ³J_{H,H} = 7.8 Hz, 4 H; CH, *o*-C₆H₄). ¹³C{¹H} NMR (100.6 MHz, CDCl₃): δ = 29.2 (CH₃, ^tBu-CN₂), 31.5 (CH₃, ^tBu-C₆H₄), 34.0 (C, ^tBu-C₆H₄), 38.7 (C, ^tBu-CN₂), 43.3 (CH₂), 120.3 (CH, *m*-C₆H₄), 125.1 (CH, *o*-C₆H₄), 143.4 (C, *p*-C₆H₄), 148.5 (C, *i*-C₆H₄), 160.9 (C, CN₂). ¹³C{¹H} NMR (100.6 MHz, C₆D₆): δ = 29.4 (CH₃, ^tBu-CN₂), 31.8 (CH₃, ^tBu-C₆H₄), 34.1 (C, ^tBu-C₆H₄), 39.0 (C, ^tBu-CN₂), 44.3 (CH₂), 121.1 (CH, *m*-C₆H₄), 125.4 (CH, *o*-C₆H₄), 143.1 (C, *p*-C₆H₄), 149.5 (C, *i*-C₆H₄), 160.7 (C, CN₂). ¹³C{¹H} NMR (100.6 MHz, [D₆]DMSO): δ = 28.8 (CH₃, ^tBu-CN₂), 31.4 (CH₃, ^tBu-C₆H₄), 33.6 (C, ^tBu-C₆H₄), 38.3 (C, ^tBu-CN₂), 42.6 (CH₂), 119.7 (CH, *m*-C₆H₄), 124.6 (CH, *o*-C₆H₄), 141.6 (C, *p*-C₆H₄), 149.0 (C, *i*-C₆H₄), 160.3 (C, CN₂). MS (ESI(+)): *m/z* (relative intensity): 491 (20) [M + H]⁺, 246 (100) [M + 2 H]²⁺. HRMS (ESI(+)): *m/z* calcd. for C₃₂H₅₁N₄ [M + H]⁺ 491.4114, found 491.4104. IR (neat, cm⁻¹): $\tilde{\nu}$ = 3446 (w, ν (N-H)), 2954 (s, ν (C-H)), 2902, 2866 (m, ν (C-H)), 1624 (vs), 1602, 1504 (s), 1458 (m), 1392 (w), 1364 (m), 1314 (w), 1282, 1270 (s), 1226 (s), 1204, 1186, 1164, 1110 (m), 1050, 1032 (w), 1012 (m), 940, 928, 903 (w), 854, 840, 812 (s), 802, 754 (m), 726 (s), 674 (m). UV/Vis (THF): λ [nm] (ϵ [L · mol⁻¹ · cm⁻¹]) 244, 2.26 × 10⁴; ≈294, 7.34 × 10³ (br shoulder).

UV/Vis spectrum of 8:^[17] UV/Vis (THF): λ [nm] (ϵ [L · mol⁻¹ · cm⁻¹]) 242, 2.89 × 10⁴ (br shoulder).

Synthesis of 9: This bis(amidine) was obtained by recrystallization from a mixture of CH₂Cl₂ (4 mL) and diethyl ether (4 mL, 1:1 v/v) at 5 °C within 3 d as a colorless crystalline solid. Yield: 66 %. Mp:

169.5–171.4 °C. Anal. Calcd for C₃₆H₄₂N₄: C, 81.47; H, 7.98; N, 10.56; found C, 81.29; H, 7.86; N, 10.73. ¹H NMR (400.1 MHz, CDCl₃): δ = 1.19 (s, 18 H; CH₃, ^tBu), 3.79 (s, 4 H; CH₂), 6.18 (broad s, 2 H; NH), 6.34 (d, ³J_{H,H} = 6.3 Hz, 4 H; CH, *o*-C₆H₄), 6.96 (d, ³J_{H,H} = 7.3 Hz, 4 H; CH, *m*-C₆H₄), 7.19–7.26 (m, 10 H; CH, Ph). ¹H NMR (400.1 MHz, C₆D₆): δ = 1.17 (s, 18 H; CH₃, ^tBu), 3.62 (s, 4 H; CH₂), 5.82 (broad s, 2 H; NH), 6.74 (d, ³J_{H,H} = 8.1 Hz, 4 H; CH, *o*-C₆H₄), 6.84–6.90 (m, 6 H; CH, *m*, *p*-Ph), 7.08 (d, ³J_{H,H} = 8.3 Hz, 4 H; CH, *m*-C₆H₄), 7.20 (d, ³J_{H,H} = 6.5 Hz, 4 H; CH, *o*-Ph). ¹H NMR (400.1 MHz, [D₆]DMSO): δ = 1.16 (s, 18 H; CH₃, ^tBu), 3.61 (s, 4 H; CH₂), 6.34 (d, ³J_{H,H} = 7.1 Hz, 4 H; CH, *o*-C₆H₄), 6.97 (d, ³J_{H,H} = 7.8 Hz, 4 H; CH, *m*-C₆H₄), 7.23–7.28 (m, 12 H; CH, Ph, NH). ¹³C{¹H} NMR (100.6 MHz, CDCl₃): δ = 31.4 (CH₃, ^tBu), 34.0 (C, ^tBu), 43.4 (CH₂), 122.5 (CH, *o*-C₆H₄), 125.0 (CH, *m*-C₆H₄), 128.2 (CH, *m*-Ph), 128.7 (CH, *o*-Ph), 129.0 (CH, *p*-Ph), 135.2 (C, *i*-Ph), 143.8 (C, *p*-C₆H₄), 147.6 (C, *i*-C₆H₄), 158.4 (C, CN₂). ¹³C{¹H} NMR (100.6 MHz, C₆D₆): δ = 31.6 (CH₃), 34.0 (C), 43.7 (CH₂), 123.2 (CH, *o*-C₆H₄), 125.6 (CH, *m*-C₆H₄), 128.3 (CH, *o*, *m*-Ph), 2 × 129.1 (CH, *p*-Ph, CH, *o*, *m*-Ph), 135.8 (C, *i*-Ph), 143.7 (C, *p*-C₆H₄), 148.8 (C, *i*-C₆H₄), 158.3 (C, CN₂). ¹³C{¹H} NMR (100.6 MHz, [D₆]DMSO): δ = 31.2 (CH₃, ^tBu), 33.5 (C, ^tBu), 41.3 (CH₂), 122.1 (CH, *o*-C₆H₄), 124.6 (CH, *m*-C₆H₄), 127.9, 128.5 (CH, *o*, *m*-Ph), 128.7 (CH, *p*-Ph), 135.2 (C, *i*-Ph), 142.2 (C, *p*-C₆H₄), 148.4 (C, *i*-C₆H₄), 157.3 (C, CN₂). MS (ESI(+)) in MeOH: *m/z* (relative intensity): 531 (30) [M + H]⁺, 266 (100) [M + 2H]²⁺. HRMS (ESI(+)): *m/z* calcd. for C₃₆H₄₃N₄ [M + H]⁺ 531.3488, found 531.3481. IR (neat, cm⁻¹): $\tilde{\nu}$ = 3272 (m, ν (N-H)), 3080, 3056, 3028 (w) 2956, 2916, 2866 (m, ν (CH)), 1616 (s), 1592 (vs), 1576 (s), 1522, 1502 (vs), 1460 (s), 1446, 1422, 1394, 1362, 1314, 1290 (m), 1252 (s), 1202, 1186, 1158, 1142, 1110, 1072 (m), 1050 (w), 1026 (m), 1014, 1002, 968, 924, 880, 862 (w), 836 (s), 772 (m), 750 (m), 696 (vs). UV/Vis (THF): λ [nm] (ϵ [L · mol⁻¹ · cm⁻¹]) 247, 3.26 × 10⁴; ≈305, 9.07 × 10³ (br shoulder).

Deprotonation Studies of 6–9: A 1.6 M solution of *n*-butyllithium in hexanes (0.06 mL, 0.10 mmol) was added dropwise to a solution of **6–9** (0.048 mmol) in THF (12 mL) at –78 °C with stirring. After 15 min, the reaction mixture was warmed to room temperature and stirred for additional 6 h (UV/Vis: 6.7 × 10⁻⁶–3.4 × 10⁻⁵ M, excitation and emission spectra: 6.0–7.5 × 10⁻³ M; see Table S35).

UV/Vis (THF): λ [nm] (ϵ [L · mol⁻¹ · cm⁻¹]) [**6**Li₂]: 240, 2.72 × 10⁴; ≈290, 9.96 × 10³ (br shoulder); [**7**Li₂]: 243, 3.15 × 10⁴; ≈293, 1.19 × 10⁴ (br shoulder); [**8**Li₂]: ≈244, 1.41 × 10⁵ (br shoulder); ≈273, 6.16 × 10⁴ (br shoulder); ≈286, 5.17 × 10⁴ (br shoulder); 311, 5.29 × 10⁴; [**9**Li₂]: 246, 1.26 × 10⁵; ≈309, 3.66 × 10⁴ (br shoulder); 412, 7.74 × 10³.

X-ray Crystallography

Single crystals of **6**, **7**, and **9**·0.8CH₂Cl₂ were obtained as colorless plates (**6**), blocks (**7**), or needles (**9**·0.8CH₂Cl₂) from slowly concentrating hexanes (**6** and **7**) or CH₂Cl₂ (**9**·0.8CH₂Cl₂) solutions at room temperature. Colorless blocks of **9**·EtOH were grown from a concentrated ethanol/acetonitrile solution at –35 °C. X-ray data for **6**, **9**·0.8CH₂Cl₂, and **9**·EtOH were collected on a Bruker D8 Venture diffractometer and for **6** on a Bruker D8 Quest X-ray diffractometer (CuK_α radiation, λ = 1.54178 Å or MoK_α radiation, λ = 0.71073 Å) by using ω and φ scans at 100 K (**6** and **9**·EtOH), 110 K (**6**) or 140 K (**9**·0.8CH₂Cl₂, Table S1 and S2). The integrated intensities for each reflection were obtained by reduction of the data frames with the program APEX3.^[28] Cell parameters were obtained and refined with 44601 (5289 unique, **6**), 34113 (3844 unique, **7**), 39871 (6376 unique, **9**·0.8CH₂Cl₂), and 17988 (3862 unique, **9**·EtOH) reflections, respectively. The integrated intensity information for each reflection was obtained by reduction of the data frames by using the SAINT algorithm of APEX3. The integrated data were corrected for absorption by using SADABS.^[29] The structures of **6**, **7**, and **9**·0.8CH₂Cl₂

were solved by direct methods and refined (weighted least-squares refinement on F^2) by using SHELXL-97.^[30] The structure of **9-4EtOH** was solved by intrinsic phasing (SHELXT) and refined on F^2 using SHELXL-2016. The hydrogen atoms were placed in idealized positions, and refined by using a riding model. In the case of **9-4EtOH**, hydrogen atoms attached to the nitrogen atoms of the bis(amidine) molecule and the solvent ethanol molecules were readily identified from the difference electron density map, and were fully refined. Non-hydrogen atoms were refined with anisotropic thermal parameters. For **9-0.8CH₂Cl₂**, elongated thermal ellipsoids on the CH₂Cl₂ atoms indicated disorder, which was modeled successfully between two positions each with an occupancy ratio of 0.67:0.13. Appropriate restraints were added to keep the bond lengths, angles, and thermal ellipsoids meaningful. For all structures, absence of additional symmetry and voids was confirmed using PLATON (ADDSYM).^[31]

Deposition Number(s) CCDC 1976262 (for **6**), 1976264 (for **7**), 1976263 (for **9-0.8CH₂Cl₂**), and 1935519 (for **9-EtOH**) contain(s) the supplementary crystallographic data for this paper. These data are provided free of charge by the joint Cambridge Crystallographic Data Centre and Fachinformationszentrum Karlsruhe Access Structures service www.ccdc.cam.ac.uk/structures.

Computational details: All structures (**6–9**) were fully geometry-optimized using TURBOMOLE v7.3.1.^[32] Density functional theory was used with the B3LYP functional,^[33] together with the RIDFT module,^[34] dispersion correction^[35] and a triple- ζ quality basis set def2-TZVP including polarization functions.^[36] No symmetry constraints were imposed on any structures during optimization. The energetic minimum of the calculated structures was confirmed by vibration analyses performed analytically (aoforce).^[37] For NMR computations, the gauge-independent atomic orbital (GIAO) method was used as implemented in TURBOMOLE v7.3.1. The B3LYP^[33] functional was used together with the RIDFT module^[34] and the basis set def2-TZVP.^[36] See Table S9 and Table S10 for selected computed ¹H NMR chemical shifts referenced to TMS.

Acknowledgments

We thank Connor O'Dea, Omar Ugarte Trejo, Nimia Zoé Maya, Ofumere Omokhodion, and Nattasith Siwabut for experimental assistance. Dr. Michael D. Walla and Dr. William E. Cotham (Mass Spectrometry Center at the University of South Carolina) are acknowledged for recording mass spectra. We are grateful to Andreas Ehnbohm for his help on computational problems. The Department of Chemistry and Biochemistry and the College of Sciences and Mathematics (CSM) at Kennesaw State University are acknowledged for financial support (New Faculty Startup Fund (No. 08020) and the CSM Research Stimulus Program). This material is based upon work supported by the National Science Foundation under Grant No. CHE-1800332.

Keywords: Amidines · Isomers · Hydrogen bonds · Density functional calculations · Luminescence

- [1] G. Häfeli, F. K. H. Kuske in *The Chemistry of Amidines and Imidates* (Eds.: S. Patai, Z. Rappoport), John Wiley & Sons, Ltd.; Chichester, UK, **1991**, pp. 1–100.
- [2] a) D. Lindauer, R. Beckert, M. Döring, P. Fehling, H. Görls, *J. Prakt. Chem.* **1995**, 337, 143–152; b) D. Lindauer, R. Beckert, T. Billert, M. Döring, H. Görls, *J. Prakt. Chem.* **1995**, 337, 508–515; c) J. Atzrodt, J. Brandenburg, C. Käßlinger, R. Beckert, W. Günther, H. Görls, J. Fabian, *J. Prakt. Chem.*

- 1997**, 339, 729–734; d) D. Müller, R. Beckert, H. Görls, *Synthesis* **2001**, 4, 601–606; e) M. Matschke, R. Beckert, L. Kubcová, C. Biskup, *Synthesis* **2008**, 18, 2957–2962; f) R. Strathausen, R. Beckert, J. Fleischhauer, D. Müller, H. Görls, *Z. Naturforsch. B* **2014**, 69, 641–649.
- [3] a) F. T. Edelmann, *Coord. Chem. Rev.* **1994**, 137, 403–481; b) J. Barker, M. Kilner, *Coord. Chem. Rev.* **1994**, 133, 219–300; c) M. P. Coles, *Dalton Trans.* **2006**, 985–1001; d) F. T. Edelmann in *Advances in Organometallic Chemistry* (Eds.: A. F. Hill, M. J. Fink), Elsevier, Amsterdam, **2008**, Vol 57, pp. 183–352; e) F. T. Edelmann, *Chem. Soc. Rev.* **2009**, 38, 2253–2268; f) S. Collins, *Coord. Chem. Rev.* **2011**, 255, 118–138; g) F. T. Edelmann in *Struct. Bonding* (Eds.: D. M. P. Mingos, P. W. Roesky), Springer, Berlin, Heidelberg, **2010**, Vol 137, pp. 109–163; h) F. T. Edelmann, *Chem. Soc. Rev.* **2012**, 41, 7657–7672; i) R. Kretschmer, *Chem. Eur. J.* **2020**, 26, 2099–2119.
- [4] a) B. S. Lim, A. Rahtu, J.-S. Park, R. G. Gordon, *Inorg. Chem.* **2003**, 42, 7951–7958; b) Z. Li, S. T. Barry, R. G. Gordon, *Inorg. Chem.* **2005**, 44, 1728–1735.
- [5] A. J. Hill, J. V. Johnston, *J. Am. Chem. Soc.* **1954**, 76, 920–922.
- [6] a) H. H. Brintzinger, D. Fischer, R. Mülhaupt, B. Rieger, R. M. Waymouth, *Angew. Chem. Int. Ed. Engl.* **1995**, 34, 1143–1170; *Angew. Chem.* **1995**, 107, 1255–1283; b) R. L. Halterman, *Chem. Rev.* **1992**, 92, 965–994; c) P. J. Shapiro, *Coord. Chem. Rev.* **2002**, 231, 67–81; d) A. H. Hoveyda, J. P. Morken, *Angew. Chem. Int. Ed. Engl.* **1996**, 35, 1262–1284; *Angew. Chem.* **1996**, 108, 1378–1401; e) Y. Qian, J. Huang, M. D. Bala, B. Lian, H. Zhang, H. Zhang, *Chem. Rev.* **2003**, 103, 2633–2690; f) S. Prashar, A. Antiñolo, A. Otero, *Coord. Chem. Rev.* **2006**, 250, 133–154; g) C. Cobzaru, S. Hild, A. Boger, C. Troll, B. Rieger, *Coord. Chem. Rev.* **2006**, 250, 189–211; h) B. Wang, *Coord. Chem. Rev.* **2006**, 250, 242–258; i) G. Erker, *Coord. Chem. Rev.* **2006**, 250, 1056–1070; j) U. Rosenthal, *Angew. Chem. Int. Ed.* **2018**, 57, 14718–14735; *Angew. Chem.* **2018**, 130, 14932–14950.
- [7] a) G. D. Whitener, J. R. Hagadorn, J. Arnold, *J. Chem. Soc., Dalton Trans.* **1999**, 1249–1255; b) M. S. Hill, P. B. Hitchcock, S. M. Mansell, *Dalton Trans.* **2006**, 1544–1553.
- [8] a) J. R. Hagadorn, J. Arnold, *Angew. Chem. Int. Ed.* **1998**, 37, 1729–1731; *Angew. Chem.* **1998**, 110, 1813–1815; b) J. R. Babcock, C. Incarvito, A. L. Rheingold, J. C. Fettinger, L. R. Sita, *Organometallics* **1999**, 18, 5729–5732; c) S. Bamber, A. Meetsma, B. Hessen, J. H. Teuben, *Organometallics* **2001**, 20, 782–785; d) J.-F. Li, L.-H. Weng, X.-H. Wei, D.-S. Liu, *J. Chem. Soc., Dalton Trans.* **2002**, 1401–1405; e) S.-D. Bai, J.-P. Guo, D.-S. Liu, *Dalton Trans.* **2006**, 2244–2250; f) J.-F. Li, S.-P. Huang, L.-H. Weng, D.-S. Liu, *J. Organomet. Chem.* **2006**, 691, 3003–3010; g) J. Wang, T. Cai, Y. Yao, Y. Zhang, Q. Shen, *Dalton Trans.* **2007**, 5275–5281; h) L. Yan, H. Liu, J. Wang, Y. Zhang, Q. Shen, *Inorg. Chem.* **2012**, 51, 4151–4160; i) A. O. Tolpygin, A. S. Shavyrin, A. V. Cherkasov, G. K. Fukin, A. A. Trifonov, *Organometallics* **2012**, 31, 5405–5413; j) G. G. Skvortsov, G. K. Fukin, S. Y. Ketkov, A. V. Cherkasov, K. A. Lyssenko, A. A. Trifonov, *Eur. J. Inorg. Chem.* **2013**, 4173–4183; k) A. O. Tolpygin, A. V. Cherkasov, G. K. Fukin, A. A. Trifonov, *Inorg. Chem.* **2014**, 53, 1537–1543; l) G. G. Skvortsov, A. O. Tolpygin, G. K. Fukin, J. Long, J. Larionova, A. V. Cherkasov, A. A. Trifonov, *Eur. J. Inorg. Chem.* **2017**, 2017, 4275–4284.
- [9] a) J. Wang, H. Sun, Y. Yao, Y. Zhang, Q. Shen, *Polyhedron* **2008**, 27, 1977–1982; b) W. Li, M. Xue, J. Tu, Y. Zhang, Q. Shen, *Dalton Trans.* **2012**, 41, 7258–7265; c) A. O. Tolpygin, G. G. Skvortsov, A. V. Cherkasov, G. K. Fukin, T. A. Glukhova, A. A. Trifonov, *Eur. J. Inorg. Chem.* **2013**, 2013, 6009–6018.
- [10] D. Osorio Meléndez, J. A. Castro-Osma, A. Lara-Sánchez, R. S. Rojas, A. Otero, *J. Polym. Sci., Part A: Polym. Chem.* **2017**, 55, 2397–2407.
- [11] J. Wang, J. Li, F. Xu, Q. Shen, *Adv. Synth. Catal.* **2009**, 351, 1363–1370.
- [12] a) M. Ohashi, A. Yagyu, T. Yamagata, K. Mashima, *Chem. Commun.* **2007**, 3103–3105; b) S. Tanaka, K. Mashima, *Inorg. Chem.* **2011**, 50, 11384–11393.
- [13] H. Kawaguchi, T. Matsuo, *Chem. Commun.* **2002**, 958–959.
- [14] M. Stollenz, *Chem. Eur. J.* **2019**, 25, 4274–4298.
- [15] C. O'Dea, O. Ugarte Trejo, J. Arras, A. Ehnbohm, N. Bhuvanesh, M. Stollenz, *J. Org. Chem.* **2019**, 84, 14217–14226.
- [16] a) E. A. Marthart, J.-B. Greving, R. Fröhlich, E.-U. Würthwein, *Eur. J. Org. Chem.* **2007**, 2007, 5071–5081; b) J.-B. Greving, H. Behrens, R. Fröhlich, E.-U. Würthwein, *Eur. J. Org. Chem.* **2008**, 2008, 5740–5754; c) J. I. Clodt, C. Wigbers, R. Reiermann, R. Fröhlich, R. E.-U. Würthwein, *Eur. J. Org. Chem.* **2011**, 2011, 3197–3209; d) C. Glotzbach, N. Gödeke, R. Fröhlich, C.-G. Daniliuc, S. Saito, S. Yamaguchi, E.-U. Würthwein, *Dalton Trans.* **2015**, 44, 9659–9671.

- [17] M. Stollenz, J. E. Raymond, L. M. Pérez, J. Wiederkehr, N. Bhuvanesh, *Chem. Eur. J.* **2016**, *22*, 2396–2405.
- [18] M. Stollenz, F. Meyer, *Organometallics* **2012**, *31*, 7708–7727.
- [19] Two NH signals at $\delta = 5.22$ ppm (major isomer) and 5.72 ppm (minor isomer) are observed for **8**; the downfield shift refers to the dominant species.
- [20] The NH resonance signal is overlaid by the Ph group signals.
- [21] Two CH₂ signals at $\delta = 3.02$ ppm (minor isomer) and 3.75 ppm (major isomer) are observed for **8**; the downfield shift refers to the dominant species.
- [22] For earlier reports about hydrogen bonds on correlations between ¹H NMR chemical shifts and crystallographic data see: a) V. Bertolasi, P. Gilli, V. Ferretti, G. Gilli, *J. Chem. Soc., Perkin Trans. 2* **1997**, 945–952; b) T. K. Harris, Q. Zhao, A. S. Mildvan, *J. Mol. Struct.* **2000**, *552*, 97–109.
- [23] V. Vass, M. Dehmel, F. Lehni, R. Kretschmer, *Eur. J. Org. Chem.* **2017**, *2017*, 5066–5073. The authors only reported an intramolecular hydrogen bond of a bis(guanidine). However, a closer inspection of the molecular structure revealed the existence of intermolecular hydrogen bonding as well ($N_{NH} \cdots N'$: 2.9500(17) Å; $N-H \cdots N'$: 2.100(19) Å; $N-H \cdots N'$: 154(2)°) that results in a polymeric arrangement of the individual bis(guanidine) molecules in a helical fashion.
- [24] *E/Z(syn/syn)* and *Z/E(syn/syn)* represent one identical pair. In total, six pairs of identical stereoisomers and four unique stereoisomers are possible for **6–9**, if each predominant tautomer retains the –NH(CH₂)₂NH–diamine core motif.
- [25] There is no evidence for the corresponding *anti* rotational isomers in the solid-state structures of **1–8**, **9**·0.8CH₂Cl₂, and **9**·EtOH.
- [26] G. A. Jeffrey, in *An Introduction to Hydrogen Bonding*, Oxford University Press, New York, **1997**.
- [27] F. H. Allen, O. Kennard, D. G. Watson, L. Brammer, A. G. Orpen, R. Taylor, *J. Chem. Soc., Perkin Trans. 2* **1987**, S1–S19.
- [28] a) APEX2: Program for Data Collection on Area Detectors; BRUKER AXS Inc., 5465 East Cheryl Parkway, Madison, WI 53711–5373 USA; b) APEX3: Program for Data Collection on Area Detectors; BRUKER AXS Inc., 5465 East Cheryl Parkway, Madison, WI 53711–5373 USA.
- [29] G. M. Sheldrick, *SADABS: Program for Absorption Correction of Area Detector Frames*; University of Göttingen, Göttingen, Germany, **2008**.
- [30] a) G. M. Sheldrick, *Acta Crystallogr., Sect. A* **2008**, *64*, 112–122; b) G. M. Sheldrick, *Acta Crystallogr., Sect. C* **2015**, *71*, 3–8.
- [31] a) A. L. Spek, *PLATON: A Multipurpose Crystallographic Tool*, Utrecht University, Utrecht, The Netherlands **2008**; b) A. L. Spek, *J. Appl. Crystallogr.* **2003**, *36*, 7–13.
- [32] a) R. Ahlrichs, M. Bär, M. Häser, H. Horn, C. Kölmel, *Chem. Phys. Lett.* **1989**, *162*, 165–169; b) F. Furche, R. Ahlrichs, C. Hättig, W. Klopper, M. Sierka, F. Weigend, *Wiley Interdiscip. Rev.: Comput. Mol. Sci.* **2014**, *4*, 91–100; c) TURBOMOLE V7.3 **2018**, A development of University of Karlsruhe and Forschungszentrum Karlsruhe GmbH, 1989–2007; TURBOMOLE GmbH, 2007. <http://www.turbomole.com>.
- [33] a) A. D. Becke, *Phys. Rev. A* **1988**, *38*, 3098–3100; b) A. D. Becke, *J. Chem. Phys.* **1993**, *98*, 5648–5652; c) C. Lee, W. Yang, R. G. Parr, *Phys. Rev. B* **1988**, *37*, 785–789.
- [34] a) K. Eichkorn, O. Treutler, H. Öhm, M. Häser, R. Ahlrichs, *Chem. Phys. Lett.* **1995**, *242*, 652–660; b) K. Eichkorn, F. Weigend, O. Treutler, R. Ahlrichs, *Theor. Chem. Acc.* **1997**, *97*, 119–124; c) M. Sierka, A. Hogekamp, R. Ahlrichs, *J. Chem. Phys.* **2003**, *118*, 9136–9148.
- [35] a) S. Grimme, *J. Comput. Chem.* **2004**, *25*, 1463–1473; b) S. Grimme, *J. Comput. Chem.* **2006**, *27*, 1787–1799; c) S. Grimme, J. Antony, S. Ehrlich, H. Krieg, *J. Chem. Phys.* **2010**, *132*, 154104.
- [36] F. Weigend, R. Ahlrichs, *Phys. Chem. Chem. Phys.* **2005**, *7*, 3297–3305.
- [37] P. Deglmann, F. Furche, R. Ahlrichs, *Chem. Phys. Lett.* **2002**, *362*, 511–518.

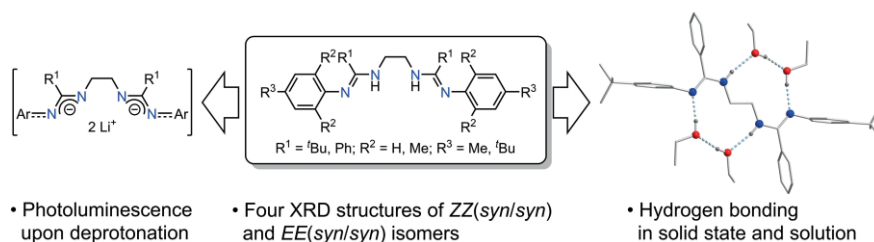
Received: February 19, 2020

Ethylene-Bridged Bis(amidines)

A. Calderón-Díaz, J. Arras, E. T. Miller,
N. Bhuvanesh, C. D. McMillen,
M. Stollenz* 1–9



Ethylene-Bridged Tetradentate Bis(amidines): Supramolecular Assemblies through Hydrogen Bonding and Photoluminescence upon Deprotonation



Flexible ethylene-bridged tetradentate bis(amidines) either encapsulate their N–H moieties through steric protection or form versatile networks of

hydrogen bonds both in the solid state and in solution. They also produce blue to green emissions upon deprotonation.

doi.org/10.1002/ejoc.202000207